

# A liquid-scintillation-based primary standardization of $^{210}\text{Pb}$

Lizbeth Laureano-Pérez\*, R. Collé, R. Fitzgerald, Iisa Outola, L. Pibida

*Physics Laboratory, National Institute of Standards and Technology, Gaithersburg, MD 20899-8462, USA<sup>1</sup>*

Received 11 May 2007; received in revised form 15 June 2007; accepted 27 June 2007

## Abstract

A new radioactivity solution standard of  $^{210}\text{Pb}$  has been developed and will be disseminated by the National Institute of Standards and Technology (NIST) as standard reference material (SRM) 4337. This new  $^{210}\text{Pb}$  solution standard is contained in a 5 mL flame-sealed borosilicate glass ampoule, consists of  $(5.133 \pm 0.002)\text{g}$  of a nominal  $1\text{mol L}^{-1}$  nitric acid solution, has a density of  $(1.028 \pm 0.002)\text{g mL}^{-1}$  at  $20^\circ\text{C}$ , has carrier ion concentrations of about  $11\mu\text{g Pb}^{2+}$  and  $21\mu\text{g Bi}^{3+}$  per gram of solution, and is certified to contain a massic activity  $(9.037 \pm 0.22)\text{kBq g}^{-1}$  as of the reference time 1200 EST, 15 June 2006. All of the uncertainties cited above correspond to standard uncertainties multiplied by a coverage factor  $k = 2$ . The standardization for the  $^{210}\text{Pb}$  content of the solution was based on  $4\pi\alpha\beta$  liquid scintillation (LS) measurements using CIEMAT/NIST  $^3\text{H}$ -standard efficiency tracing (CNET). Confirmatory determinations were also performed by high-resolution HPGe  $\gamma$ -ray spectrometry, by  $2\pi\alpha$  spectrometry with a Si surface barrier detector of separated  $^{210}\text{Po}$ , and by  $4\pi\beta(\text{LS})-\gamma(\text{NaI})$  anticoincidence counting.

Published by Elsevier Ltd.

**Keywords:** Anticoincidence counting; Beta counting; CIEMAT/NIST method; Efficiency tracing; Lead-210; Liquid scintillation (LS); Radioactivity; SRM; Standards

## 1. Introduction

This paper describes the development of a  $^{210}\text{Pb}$  solution standard at the National Institute of Standards and Technology (NIST). It is a new and important complement to the suite of radioactivity standard reference materials (SRM) available from NIST. The standard, SRM 4337, is intended primarily for the calibration of instruments that are used to measure radioactivity and for the monitoring of radiochemical procedures which are used in a variety of applications. Such a standard is widely needed and has been often requested by the worldwide environmental radioactivity measurement community.

The isotope  $^{210}\text{Pb}$  is a longer-lived  $[(22.20 \pm 0.22)\text{a}]$ , intermediate member of the naturally occurring  $^{238}\text{U}$  radioactive decay series, and is widely distributed in the

environment. Its measurement is used as a monitor for natural uranium contamination, for short-term geological dating, and for  $^{238}\text{U}/^{226}\text{Ra}/^{210}\text{Pb}$  decay-chain equilibrium/disequilibrium studies.

Fig. 1, based on National Nuclear Data Center compilations (ENSDF, 2006), shows the decay scheme for the  $^{210}\text{Pb}$  subseries. As indicated,  $^{210}\text{Pb}$  decays by  $\beta^-$  emission to  $^{210}\text{Bi}$  through two branches. The first, having a decay probability of  $I_\beta = 0.84 \pm 0.03$ , is to the 46.54 keV isomeric state in  $^{210}\text{Bi}$  [ $E_{\beta(\text{max})} = (17.0 \pm 0.5)\text{keV}$ ;  $E_{\beta(\text{ave})} = (4.16 \pm 0.13)\text{keV}$ ]. The second,  $I_\beta = 0.16 \pm 0.03$ , is to the  $^{210}\text{Bi}$  ground state [ $E_{\beta(\text{max})} = (63.5 \pm 0.5)\text{keV}$ ;  $E_{\beta(\text{ave})} = (16.16 \pm 0.13)\text{keV}$ ]. Both branches are first forbidden, non-unique beta decay transitions, with poorly known shape factors (Behrens and Szybisz, 1976). The  $^{210}\text{Bi}$  isomeric transition is highly converted ( $\alpha_{\text{tot}} = 18.7$ ;  $\alpha_{\text{L}} = 14.2$ ;  $\alpha_{\text{M}} = 3.36$ ) with only 4.25% of the  $^{210}\text{Pb}$  decay occurring by the 46.54 keV  $\gamma$ -ray. The shorter-lived  $[(5.012 \pm 0.005)\text{d}]$   $^{210}\text{Bi}$  decays by another, but much higher energy, first forbidden, non-unique  $\beta^-$  transition to the ground state of  $^{210}\text{Po}$  [ $E_{\beta(\text{max})} = (1161.5 \pm 1.5)\text{keV}$ ;

\*Corresponding author. Tel.: +1 301 975 8797; fax: +1 301 926 7416.

E-mail address: [lizbeth.laureano-perez@nist.gov](mailto:lizbeth.laureano-perez@nist.gov) (L. Laureano-Pérez).

<sup>1</sup>The National Institute of Standard and Technology is an agency of the Technology Administration of the US Department of Commerce.

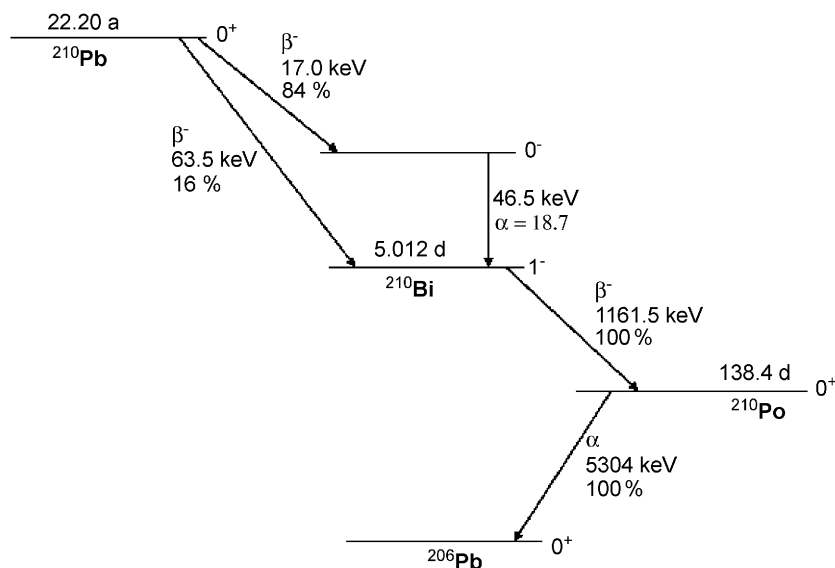


Fig. 1. Decay scheme for the  $^{210}\text{Pb}$  decay subseries, derived from National Nuclear Data Center compilations (ENSDF, 2006).

$E_{\beta(\text{ave})} = 389.0 \pm 0.4 \text{ keV}$ ]. The subseries ends with the alpha decay of  $(138.376 \pm 0.002) \text{ d}$   $^{210}\text{Po}$  to stable  $^{206}\text{Pb}$  [ $E_{\alpha} = (5304.33 \pm 0.07) \text{ keV}$ ].<sup>2</sup>

## 2. Experimental methods, results, and discussion

### 2.1. Overview

The  $^{210}\text{Pb}$  standardization described herein was performed from June to December 2006 on SRM ampoules that were prepared in December 1999. Fig. 2 illustrates the scheme used to prepare the standards and various counting sources that were employed for the standardization and confirmatory measurements. The certified  $^{210}\text{Pb}$  massic activity for the standards was obtained from a primary standardization based on  $4\pi\alpha\beta$  liquid-scintillation (LS) counting. Additional measurements, for confirmatory purposes, were performed by high-resolution HPGe  $\gamma$ -ray spectrometry, by  $2\pi\alpha$  spectrometry with a Si surface-barrier detector for determination of  $^{210}\text{Po}$  separated from the  $^{210}\text{Pb}$  solutions, and by  $4\pi\beta(\text{LS})-\gamma(\text{NaI})$  anticoincidence counting.

### 2.2. Preparation of master solution and SRM ampoules

A  $^{210}\text{Pb}$  master solution was prepared at NIST in December 1999 (Lucas, 2005), and was a gravimetrically linked dilution of a  $^{210}\text{Pb}$  source obtained from the Czech Metrological Institute (CMI). The master solution contains

approximately 11  $\mu\text{g}$  of  $\text{Pb}^{2+}$  and 21  $\mu\text{g}$  of  $\text{Bi}^{3+}$  per gram of solution in  $1 \text{ mol L}^{-1}$   $\text{HNO}_3$ , whose density was determined to be  $(1.028 \pm 0.002) \text{ g mL}^{-1}$  at  $20^\circ\text{C}$ . Nominal 5 mL aliquants of the master solution were dispensed into standard NIST, 5 mL, borosilicate-glass SRM ampoules (NIST, 2007). The average solution mass per ampoule, as determined from the dispensed mass difference (filled and empty), was  $(5.133 \pm 0.002) \text{ g}$  and was based on measurements of 18 ampoules (about every 5–10 apart in sequence) from a set of 105 ampoules. After filling, the SRM ampoules were flame-sealed and sterilized by autoclaving at about 200 kPa for 20 min.

### 2.3. Photonic-emission impurity analyses

Analyses for photon-emitting impurities were performed using two different high-purity intrinsic germanium detectors: B-detector ( $L = 54 \text{ mm}$ ;  $\phi = 55 \text{ mm}$ ) and X-detector ( $L = 36 \text{ mm}$ ;  $\phi = 44 \text{ mm}$ ). Both detectors are n-type coaxial detectors with 0.5 mm Be windows. They are housed in 10 cm thick lead shields with graded cadmium/copper absorbers, and are calibrated for energy and detection efficiency in standard geometries using a large number of standardized sources (ANSI, 1999). The detectors and spectrometry procedures used by NIST have been described by Pibida et al., (2006, 2007).

Measurements with both detectors were made on the  $^{210}\text{Pb}$  SRM ampoules in several standard source geometries for counting periods of 24 h. Two or three replicate trials were performed for each geometry–detector combination. The results of these measurements were also used to perform confirmatory  $^{210}\text{Pb}$  activity determinations (see Section 2.5.1).

No impurity photons were detected in any of 10 counting trials. Lower limits, expressed as massic photon emission

<sup>2</sup>All of the uncertainties on the decay data cited above correspond to assumed  $k = 1$  standard uncertainties; whereas all of the uncertainties on the properties of SRM 4337 that follow correspond to expanded uncertainty intervals with a coverage factor of  $k = 2$ , which are calculated and reported according to ISO (1993) and NIST (Taylor and Kuyatt, 1994) guidelines.

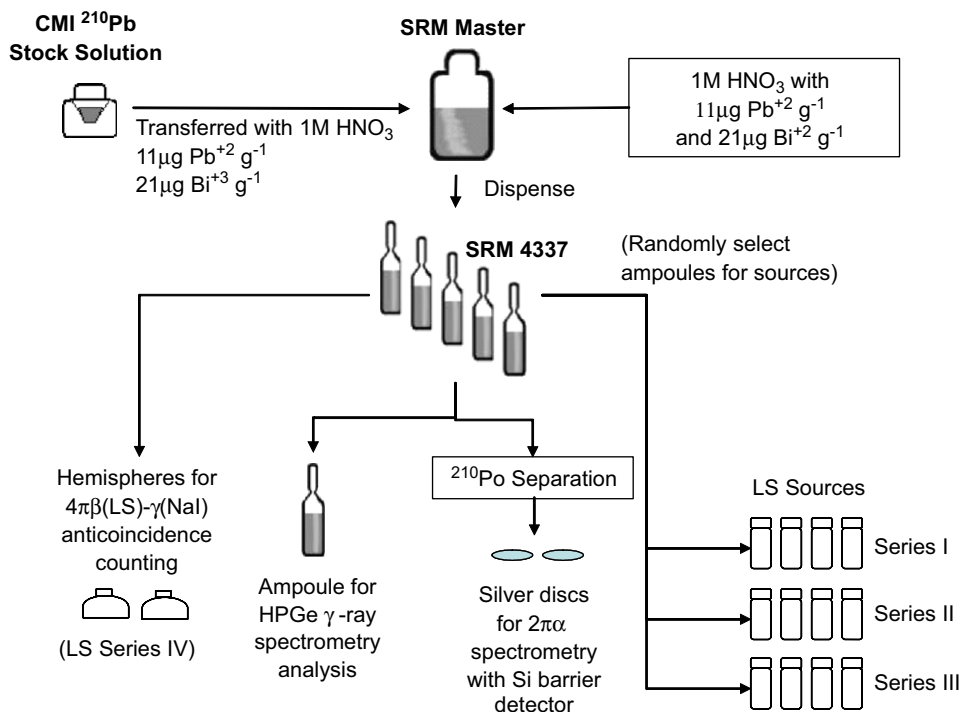


Fig. 2. Scheme for preparation of the  $^{210}\text{Pb}$  solution standards (SRM 4337) and the counting sources used for the  $4\pi\beta$  LS-based standardization and confirmatory measurements.

rates, on 15 June 2006, were:

$$1.7\text{ s}^{-1}\text{ g}^{-1} \text{ for the energy region } 20\text{ keV} < E < 60\text{ keV},$$

$$0.3\text{ s}^{-1}\text{ g}^{-1} \text{ for the energy region } 60\text{ keV} < E < 1800\text{ keV}.$$

The relative standard uncertainty contribution to the certified  $^{210}\text{Pb}$  massic activity due to photon-emitting impurities was estimated to be equal to the estimated limit of detection for the impurities (see Section 2.4.5).

## 2.4. LS-based primary standardization

### 2.4.1. CNET methodology

The LS-based standardization was based on the CIEMAT/NIST  $^3\text{H}$ -standard efficiency tracing (CNET) method,<sup>3</sup> obtained with the CN2003 code of Gunther (2002, 2003). Complementary efficiency calculations for the  $^{210}\text{Pb}$  and  $^{210}\text{Bi}$   $\beta$  transitions were also performed with the CIEMAT-developed EFFY4 code.<sup>4</sup> Features of this method have been described in numerous publications by the CIEMAT/NIST originators (Grau Malonda and Garcia-Torano, 1982; Coursey et al., 1985, 1986). The

method as currently employed at NIST is based on well-established procedures that are somewhat routine for this laboratory and which have been described in detail by Collé and Zimmerman (1996a, b, 1997) and Zimmerman and Collé (1997a, b). An appendix in the first paper cited here (Collé and Zimmerman, 1996a) includes an outline and schematic representation of the measurement process as well as a discussion of its theoretical basis and practical implementation. The specific analysis procedure used for this work is similar to that described in many previous publications by Collé (1997a, b, c, 1999, 2000, 2001).

The nuclear data for the  $^{210}\text{Pb}$  subseries nuclides that were used as input for the tracing codes were summarized in Section 1 above. The relevant nuclear data for the tracing nuclide  $^3\text{H}$  were super allowed ( $1/2^+ \rightarrow 1/2^+$ ) transition to the ground state of  $^3\text{He}$ ;  $I_\beta = 1$ ;  $E_{\beta(\text{max})} = (18.594 \pm 0.008)\text{ keV}$ ;  $E_{\beta(\text{ave})} = (5.69 \pm 0.04)\text{ keV}$ ;  $(12.32 \pm 0.02)$  a half-life, as taken from ENSDF (2006) and as based on a 1998 evaluation. A more recent evaluation by Chechev (2006) lists values for  $E_{\beta(\text{max})}$  and the half-life that differ by 0.16% and 0.06%, respectively. These newer values have a negligible effect on the tracing results.

A large aspect of the experimental design for the CNET method as employed here is to randomize as many experimental variables as possible to ensure that to the  $^{210}\text{Pb}$  massic activity determination is not biased by one set of chosen conditions. The randomized experimental conditions include cocktail composition (scintillant, aqueous fraction, acid and carrier ion concentrations in the aqueous

<sup>3</sup>The acronym CIEMAT/NIST refers to the two laboratories that collaborated in developing the protocol for this LS tracing methodology; viz., the Centro de Investigaciones Energéticas, Medioambientales y Tecnológicas (CIEMAT) and the National Institute of Standards and Technology (NIST).

<sup>4</sup>This is an updated and revised version of the EFFY code. Refer to Garcia-Torano and Grau Malonda (1985), Grau Malonda et al. (1985) and Garcia-Torano (1993).

Table 1  
LS cocktail compositions used for the standardization of  $^{210}\text{Pb}$

Cocktail series	Scintillant	$N_s$	$M/\text{g}$	$f_w$	$C_a/(\text{mol L}^{-1})$	$C_{\text{Pb}}/(\mu\text{g g}^{-1})$
1	HS	11	9.0	0.1	0.06	0.69
2	PCS	7	9.2	0.02	0.30	3.3
3	PCS	7	8.9	0.06	0.09	0.95
4	PCS	4	3.7	0.06	0.64	7.0

Series 1–3 were used for the  $4\pi\alpha\beta$  LS measurements with  $^3\text{H}$ -standard efficiency tracing; series 4 was used for the  $4\pi\beta\text{--}\gamma$  anticoincidence counting experiments.

$N_s$ , number of samples in each series;  $M$ , mass of scintillation fluid in each cocktail (in grams);  $f_w$ , aqueous mass fraction in cocktail;  $C_a$ ,  $\text{HNO}_3$  concentration (in  $\text{mol L}^{-1}$ ) in aqueous fraction of cocktail;  $C_{\text{Pb}} = \text{Pb}^{2+}$  ion concentration (in  $\mu\text{g g}^{-1}$ ) in aqueous fraction of cocktail. The  $\text{Bi}^{3+}$  ion concentration is 1.9 times that of  $\text{Pb}^{2+}$ .

part), LS counter, counting condition, measurement time, and the tracing code with its variables.

#### 2.4.2. LS cocktails

A test using three different commercially available, environmentally “safe”, “biodegradable” scintillants<sup>5</sup> was performed in order to evaluate the stability of various cocktail compositions with time. The scintillants were:

- Ready Safe (Beckman Coulter, Fullerton, CA, USA), designated as RS;
- Insta-Gel plus (Perkin Elmer, Waltham, MA, USA), designated as IG; and
- OptiPhase HiSafe3 (Perkin Elmer, formerly Wallac, Finland), designated as HS.

They were used to prepare a matrix of compositions with varying aqueous mass fraction, ranging from 0.06 to 0.1, and carrier ion content, ranging from 0.7 to  $15 \mu\text{g}$  of  $\text{Pb}^{2+}$  per gram of the aqueous fraction (the  $\text{Bi}^{3+}$  ion content scaled in all cases with  $\text{Pb}^{2+}$  by a factor of  $\text{Bi}^{3+}/\text{Pb}^{2+} = 1.9$ ). Every composition was found to be unstable to some extent or other, where changes in the LS counting rates varied from about 0.002% per day to over 0.03% per day over the course of 3 days. Based on these results, cocktails prepared with the di-isopropylnaphthalene-based HS scintillant and having high carrier fractions were found to be the most stable. This composition was then selected for use in preparing a first series of cocktails. Because even the best performing HS composition cocktails had disappointing stability, two further series of LS cocktails were prepared with PCS (Amersham Biosciences, Sweden). This is a “non-safe,” xylene-based scintillation fluid, which was thought to be able to produce more stable cocktails based on the past experience (Collé, 1997c).

The cocktail compositions for these three series are summarized in Table 1. The cocktails were prepared from randomly selected ampoules in the set of SRM 4337

ampoules. The cocktails were characterized in terms of the aqueous mass fraction  $f_w$ , the  $\text{HNO}_3$  acid concentration in the aqueous part  $C_a$ , and the  $\text{Pb}^{2+}$  ion concentration  $C_{\text{Pb}}$  in the aqueous part. Series 1–3 were contained in 20 mL glass LS vials fitted with polyethylene lined plastic caps and were used for the CNET measurements, while the series 4 cocktails were contained in specially-fabricated, glass “pseudo-hemispheres” for the  $4\pi\beta\text{--}\gamma$  anticoincidence counting (see Section 2.5.3). Each of the first three series consisted of 7–11 sources, identically matched in terms of composition and quenching (before the addition of an imposed quenching agent). An equal number of composition-matched  $^3\text{H}$  cocktails were prepared using a gravimetric dilution of NIST tritiated-water standard SRM 4927F (NIST, 2000). These  $^3\text{H}$  LS sources were matched with the  $^{210}\text{Pb}$  sources in terms of acid composition and ion concentration by the addition of non-radioactive carrier solutions. The sources consisted of an appropriate aliquant of either  $^{210}\text{Pb}$  or  $^3\text{H}$  solution, approximately 9 mL of one of the commercial LS scintillants, and an aqueous fraction range of 0.02–0.1. Varying masses of an imposed chemical quenching agent, consisting of a 10% solution of nitromethane ( $\text{CH}_3\text{NO}_2$ ) in ethanol, were added to the  $^3\text{H}$  and  $^{210}\text{Pb}$  cocktails within a given series to vary the LS detection efficiencies over a wide range. Blank sources for background subtraction were composed of scintillant, carrier solution (to match acid and ion compositions), and nitromethane (to match chemical quenching). All mass additions of radioactive aliquants ( $^{210}\text{Pb}$  and  $^3\text{H}$ ), typically 50–100 mg, were performed with a microbalance using polyethylene aspiration-type pycnometers.

#### 2.4.3. LS spectrometers

Three different instruments were used for the LS measurements. They have considerably different operating characteristics (e.g., low-energy threshold, deadtime, linear vs. logarithmic energy binning, etc.), which helps to ensure that any standardization results are independent of the instrumental conditions.

The LS spectrometers were

- (i) Packard TriCarb A2500TR (Perkin-Elmer, Wesley, MA);

<sup>5</sup>Certain commercial equipment, instruments and materials are identified in this paper to foster understanding. Such identification does not imply recommendation or endorsement by NIST, nor does imply that the materials and/or equipment are the best available for the purpose.

Table 2  
Results for the massic activity for SRM 4337, at a Reference Time of 1200 EST 15 June 2006, as obtained from the  $4\pi\alpha\beta$  LS measurements with  $^3\text{H}$  standard efficiency tracing

Cocktail series	Instrument	Age/d	$N_d$	$\varepsilon_3$	$\varepsilon_A$	$\varepsilon_B$	$A/(\text{kBq g}^{-1})$	$s/\%$
1	P	1	33	0.39–0.30	0.92–0.90	0.989–0.987	9.037	0.029
	B	4	33	0.43–0.37	0.93–0.92	0.991–0.990	9.044	0.008
	W	12	33	0.36–0.30	0.92–0.90	0.990–0.988	9.041	0.014
	P	14	33	0.36–0.30	0.92–0.90	0.990–0.988	9.030	0.021
	P	19	55	0.36–0.30	0.92–0.90	0.990–0.988	9.030	0.031
	W	28	33	0.36–0.30	0.92–0.90	0.990–0.988	9.046	0.027
2	P	2	35	0.40–0.25	0.92–0.89	0.991–0.986	9.034	
	W	6	21	0.40–0.25	0.92–0.89	0.991–0.986	9.039	
	B	12	21	0.47–0.31	0.93–0.91	0.992–0.988	9.041	0.026
	P	16	35	0.39–0.23	0.92–0.89	0.990–0.985	9.032	0.056
3	P	2	35	0.36–0.22	0.92–0.88	0.990–0.984	9.036	0.035
	W	6	21	0.36–0.22	0.92–0.88	0.990–0.984	9.044	0.014
	B	12	21	0.43–0.28	0.93–0.90	0.991–0.987	9.042	0.026
	P	16	35	0.36–0.20	0.92–0.87	0.990–0.983	9.026	0.034
All	Unweighted grand mean						9.037	—
All	Relative standard deviation of grand mean ( $n = 14$ )						—	0.067

Refer to Table 1 for LS cocktail compositions of the series.  
Instrument refers to LS counter used: W, Wallac; B, Beckman; P, Packard.  
Age is the approximate time between LS cocktail preparation and the middle of the counting cycles, in days.  
 $N_d$  is the number of determinations, given by the product of the number of sources in the series (Table 1) and number of counting cycles.  
 $\varepsilon_3$ ,  $\varepsilon_A$ , and  $\varepsilon_B$  is the range of values for the  $^3\text{H}$ ,  $^{210}\text{Pb}$  and  $^{210}\text{Bi}$  LS efficiencies, respectively, in the series of quenched cocktails.  
 $A$  is the massic activity in units of  $\text{kBq g}^{-1}$  at the reference time 1200 EST 15 June 2006.  
 $s$  is the relative standard deviation (for  $N_d$  determinations), in percent.

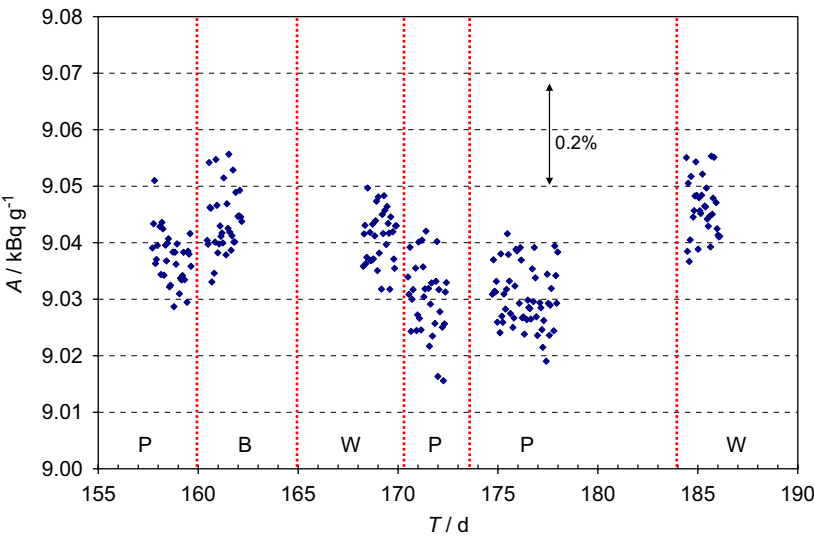


Fig. 3. Measurement results for the massic activity  $A$  (in units of  $\text{kBq g}^{-1}$ , at a 1200 EST 15 June 2006 reference time) of the  $^{210}\text{Pb}$  solution standards as a function of time  $T$  (2006 Julian day numbers) for cocktail series I (see Table 1) as obtained on six separate measurement occasions with the three LS counters (P = Packard; B = Beckman; W = Wallac). The series contained 11 varyingly quenched  $^{210}\text{Pb}$  cocktails (and an equal number of composition matched  $^3\text{H}$  cocktails) and was measured for either three or five cycles on each of the 6 occasions, resulting in 220 determinations.

- (ii) Wallac 1414 Winspectral (Perkin-Elmer, Wesley, MA); and
- (iii) Beckman LS 6500 (Beckman Coulter, Fullerton, CA).

They are designated as P, W, and B, respectively (see Table 2 and Fig. 3). All three counters operate at ambient temperature, employ two photomultiplier tubes (PMTs) in

a sum-coincidence mode, and determine lifetime counting intervals with gated oscillators. The detection thresholds for all three instruments are very, very nominally 1 keV, although they are known to be somewhat different. Spectral data from the P instrument are processed and stored linearly; whereas that from W and B are stored logarithmically (logarithmic signal amplification in W;



logarithmic analog-to-digital converter (ADC) in B). Each instrument uses a slightly different quench determination method with an external  $\gamma$ -ray source and an internally derived quench indicating parameter (QIP). These QIP values are used to account for slight quench differences between the composition-matched  $^{210}\text{Pb}$  and  $^3\text{H}$  cocktails (Collé, 1997b). The QIP employed by B is the Horrocks number  $H$ , which is determined by the downward spectrum shift of the Compton edge of the external  $^{137}\text{Cs}$  source with increasing quenching in a cocktail. The value of  $H$  corresponds to the spectral channel number shift between the quenched cocktail and an unquenched blank reference cocktail. The channel number shift  $H = (c_1 - c_2)$  is proportional to the logarithmic energy ratio  $H \propto \log(E_1/E_2)$  because of the logarithmic pulse amplification in this instrument. Both the P and W instruments utilize proprietary mathematical algorithms to derive a QIP from energy distribution transforms of the Compton spectra from their respective external  $\gamma$ -ray sources ( $^{133}\text{Ba}$  in P;  $^{152}\text{Eu}$  in W). They are called, respectively, the transformed Spectral Index of the External Standard  $tSIE$  and the External Standard Quench Parameter  $SQP(E)$ .

#### 2.4.4. $4\pi\alpha\beta$ LS-based standardization result

Three distinct sets of LS measurements were performed, corresponding to the three sets of cocktails. The counting arrangement used for each set consisted of interspersing the matched pairs of  $^{210}\text{Pb}$  and  $^3\text{H}$  cocktails into the counters, with at least two blanks positioned at certain intervals within the series. The counting time was typically 30 min per sample for 3–5 cycles per measurement occasion. The measurements were performed under the assumption that the  $^{210}\text{Pb}$  subseries nuclei were in secular equilibrium. Each cocktail series was counted on several measurement occasions, cycling through measurements on all three counters. Invariably, the sources for a given series were measured on more than one occasion in at least one counter. The measurements for a given series were conducted over periods ranging from about 18–30 days, which was sufficiently long to observe possible  $^{210}\text{Pb}$ – $^{210}\text{Bi}$ – $^{210}\text{Po}$  series disequilibria that might have occurred in the solutions during preparation of the cocktails. Fig. 3 shows the results for the 220 determinations of the  $^{210}\text{Pb}$  massic activity (at a 1200 EST 15 June 2006 reference time) as derived from measurements obtained on six separate occasions over the course of 29 days with the series I cocktails. As indicated, the cocktails were counted on three separate occasions with the Packard (P) counter, on two occasions with the Wallac (W), and once with the Beckman (B) instrument. It is apparent from Fig. 3 that there is an evident between-measurement-occasion component of variance. The largest difference between any one determination and the average value was 0.25%, which indicated that there was excellent precision for this cocktail series despite the wide variation in conditions.

The traced massic activity values  $A = R/\varepsilon_{\text{total}}$  were derived from the background- and decay-corrected massic LS counting rates  $R$ , after normalization for the aliquant mass. The total LS efficiency is given by the sum of the contribution from the three nuclides in the subseries, normalized by the Bateman (1910) coefficients under the assumption of radioactive equilibrium, i.e.,

$$\varepsilon_{\text{total}} = \varepsilon_A + \frac{\lambda_B}{(\lambda_B - \lambda_A)} \varepsilon_B + \frac{\lambda_B \lambda_C}{(\lambda_B - \lambda_A)(\lambda_C - \lambda_A)} \varepsilon_C, \quad (1)$$

where  $\lambda_A$ ,  $\lambda_B$  and  $\lambda_C$  are the decay constants for  $^{210}\text{Pb}$ ,  $^{210}\text{Bi}$  and  $^{210}\text{Po}$ , respectively; and where  $\varepsilon_A$ ,  $\varepsilon_B$  and  $\varepsilon_C$  are the  $^{210}\text{Pb}$ ,  $^{210}\text{Bi}$ , and  $^{210}\text{Po}$  LS detection efficiencies. Substitution of the respective half-life values (Section 1) yields

$$\varepsilon_{\text{total}} = \varepsilon_A + (1.0006185 \pm 0.0000061)\varepsilon_B + (1.01799 \pm 0.00018)\varepsilon_C. \quad (2)$$

The detection efficiency  $\varepsilon_C$  for the  $^{210}\text{Po}$  was taken to be 0.998 since the detection of an alpha particle is practically 100% for any LS counter under almost all quench conditions, excepting for an approximate 0.2% wall effect (Cassette, 2002). The efficiencies  $\varepsilon_A$  and  $\varepsilon_B$  were obtained from tracing against measured  $^3\text{H}$  efficiencies  $\varepsilon_3$  and calculated with the CN2003 code (Gunther, 2003). Refer to Collé and Zimmerman (1996a) for the stepwise procedure used to account and correct for small quench differences through the use of measured QIP values and to link the measured  $\varepsilon_3$  values to calculated  $\varepsilon_A$  and  $\varepsilon_B$  efficiencies. Fig. 4 shows the relationship between the  $^{210}\text{Pb}$ ,  $^{210}\text{Bi}$  and  $^3\text{H}$  detection efficiencies as obtained with the CN2003 code of Gunther (2003).

The standardization results, in terms of the  $^{210}\text{Pb}$  massic activity decay corrected to 1200 EST 15 June 2006, of 14 counting trials obtained with the three series of cocktails are given in Table 2. They represent 444 determinations of the massic activity for  $^{210}\text{Pb}$  SRM 4337 solution obtained under a variety of conditions: three cocktail compositions using two different scintillants; 7–11 sources in each series; each source measured three to five times on a given measurement occasion; multiple measurement occasions with different LS spectrometers. The standardization covered efficiency-tracing quenching ranges that corresponded to  $^{210}\text{Pb}$  detection efficiencies ( $\varepsilon_A$ ) from 0.87 to 0.93,  $^{210}\text{Bi}$  ( $\varepsilon_B$ ) detection efficiencies of 0.983–0.992, and  $^3\text{H}$  efficiencies ( $\varepsilon_3$ ) from 0.20 to 0.47. The unweighted grand mean of the 14 trials given in Table 2 was used as the certified massic activity,

$$A = 9.037 \text{ kBq g}^{-1} \pm 2.4\% \text{ at } 1200, \text{ EST } 15 \text{ June, } 2006$$

for SRM 4337, where the stated relative uncertainty corresponds to a combined standard uncertainty multiplied by a coverage factor  $k = 2$  (see Section 2.4.5).<sup>6</sup> The 14

<sup>6</sup>The 2.4 % uncertainty on  $A$  results in an interval of  $0.22 \text{ kBq g}^{-1}$ . Hence, the massic activity value and its uncertainty interval, as given in the SRM 4337 Certificate is unbalanced in terms of the number of place values, i.e.,  $(9.037 \pm 0.22) \text{ kBq g}^{-1}$ . This practice generally violates NIST uncertainty guidelines in that uncertainties should not be reported with greater than two significant figures and the number of place values for the

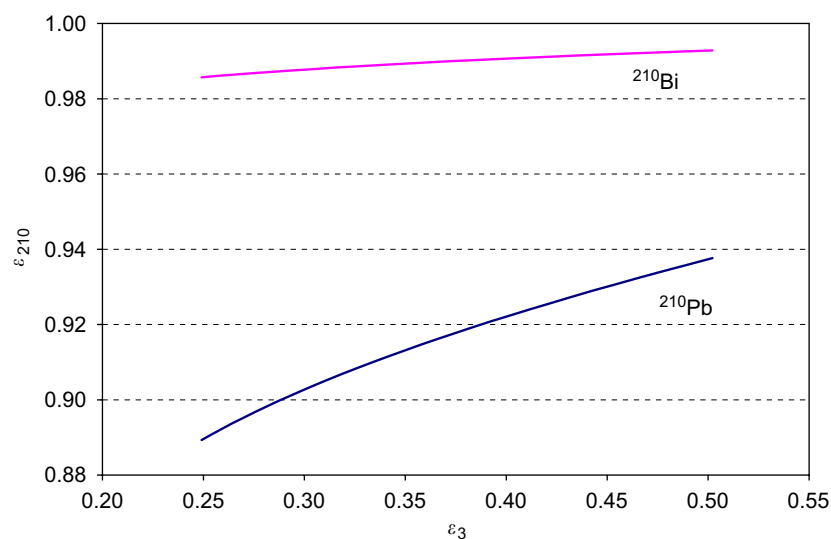


Fig. 4. CN2003-code calculations for the  $^{210}\text{Pb}$  and  $^{210}\text{Bi}$  LS detection efficiencies as a function of that for  $^3\text{H}$  over the range of typical experimental efficiencies.

individual data sets, each having  $n = 21\text{--}55$  determinations, were tested for normality with Dataplot (2007) and all results from series 1 to 3 could accept the normality assumption at a 95% and 99% level; those sets using series 2 cocktails generally did not “pass,” presumably because of low-water fraction effects on cocktails having high surfactant contents (Collé and Zimmerman, 1997). All individual trial averages were consistent having relative standard deviations ranging from 0.007 to 0.056% for  $\nu = 20\text{--}54$  degrees of freedom. The average values of the 14 data sets also passed a normality test at a 99% level and the grand mean had a relative standard deviation (corresponding to a relative standard deviation of the mean for  $\nu = 13$  degrees of freedom) of 0.067%.

The  $^{210}\text{Pb}$  massic activity is strongly dependent on the  $^{210}\text{Pb}$  efficiency ( $\varepsilon_A$  in Eq. (2)) as obtained from the CN2003-code tracing calculations, and less so for the  $^{210}\text{Bi}$  and  $^{210}\text{Po}$  efficiencies ( $\varepsilon_B$  and  $\varepsilon_C$ ) because of their very large (near 100%) values. To evaluate the effect of the code results for the lower-energy  $^{210}\text{Pb}$   $\beta$  transitions, ancillary calculations were performed using the EFFY4 code (Garcia-Torano, 1993). Fig. 5, a plot of the ratio  $\varepsilon_{\text{EFFY}}/\varepsilon_{\text{CN}}$  vs.  $\varepsilon_{\text{CN}}$ , illustrates the detection efficiency difference obtained with the two codes for just the  $\beta$  detection part of the total  $^{210}\text{Pb}$  LS efficiency. As indicated, there is about a 0.5–0.7% difference in the two results in the mid-range of efficiencies. This manifests into a change of about 0.1% in the total LS efficiency  $\varepsilon_{\text{total}}$  for the  $^{210}\text{Pb}$  subseries. This type of code dependence was previously observed for  $^{63}\text{Ni}$  (Collé, et al., 2007b). Even for this higher energy, allowed  $\beta$  transition ( $E_{\beta(\text{max})} = 66.945$  keV), the calculated efficiencies

from the two codes differed by about 0.4%. The difference in the calculated  $^{210}\text{Pb}$   $\beta$  efficiencies obtained with CN2003 and EFFY4 cannot be attributed to differences in the calculated beta spectra used in the codes. Typical spectra obtained with either code are shown in Fig. 6. The spectra from the two codes were not only in excellent agreement, but both also agreed with results from the BETAENG6 code of Cassette (2006) and the SIMPBETA code of Michotte (2006). Since no differences could be found in the computed  $^{210}\text{Pb}$  beta spectra for the two codes, the computed detection efficiency differences were, therefore, attributed to the use of different ionization quenching functions  $Q(E)$  in the two codes. The EFFY4 code used a formula obtained by Los Arcos et al. (1987) for toluene (see also Grau Malonda, 1999); whereas our use of the default conditions for the CN2003 code employed a  $Q(E)$  approximation of Los Arcos and Ortiz (1997) applicable for a di-isopropylnaphthalene-based scintillation fluid, like the HiSafe3 used for the series 1 cocktails. Neither code should be expected to be perfectly correct for xylene-based PCS cocktails used in the series 2 and 3 cocktails.

#### 2.4.5. Uncertainty assessment

The relative combined standard uncertainty in the  $^{210}\text{Pb}$  massic activity for SRM 4337 at a reference time of 1200 EST, 15 June 2006 is 1.2%. The relative expanded uncertainty, using a coverage factor of  $k = 2$ , is 2.4%, which is assumed to provide an approximate 95% level of confidence. The component uncertainties used to obtain these estimates are outlined in Table 3, as taken directly from the SRM 4337 Certificate (NIST, 2006). The components, following the usual ISO and NIST guidelines (ISO, 1993; Taylor and Kuyatt, 1994), are divided into categories for the type of assessment: type A for those determined by statistical methods; and type B for those determined by other methods. The combined type-A assessment components (items 1 and 2 in Table 3) were

(footnote continued)

certified quantity and its uncertainty should match. The imbalance was accepted here to maintain the four significant precision that is traditional for certified activities in radioactivity SRMs, which typically have uncertainties considerably less than 2.4 %.

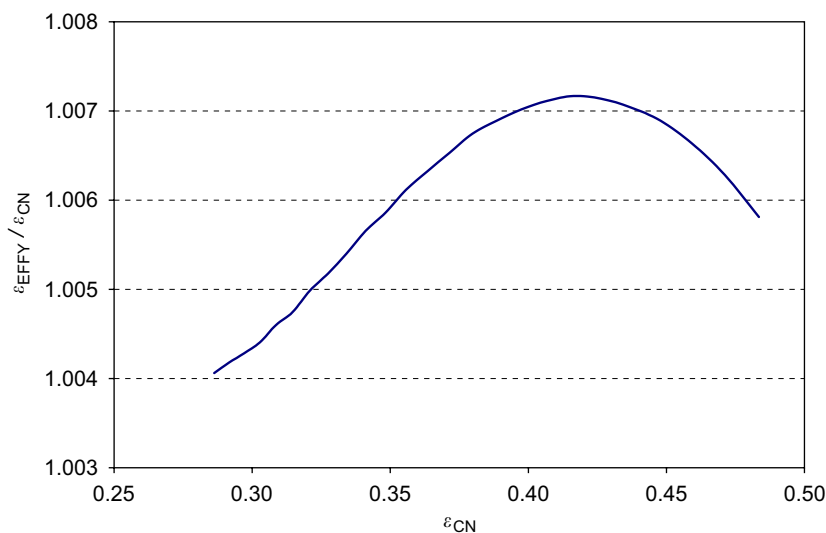


Fig. 5. Comparison of the computed LS efficiency for the  $^{210}\text{Pb}$   $\beta$  transitions as obtained with the *EFFY4* and *CN2003* codes. The efficiency ratio  $\epsilon_{\text{EFFY}}/\epsilon_{\text{CN}}$  plotted against  $\epsilon_{\text{CN}}$  reflects only that part of the total LS efficiency due to just the two  $^{210}\text{Pb}$   $\beta$  transitions. The difference between  $\epsilon_{\text{CN}}$  given here and the total  $^{210}\text{Pb}$  LS efficiency in Fig. 4 is the contribution due to the X-rays and electrons (conversion + Auger) from the 46.5-keV isomeric transition in  $^{210}\text{Bi}$ .

derived from multiple-way classification techniques (Snedecor and Cochran, 1967) for subgroupings of the results by within- and between-measurement occasion, by cocktail series, and by LS spectrometers.

The major contributors to the overall uncertainty are threefold. The first and largest (1.1%) is the standard uncertainty for the  $^{210}\text{Pb}$  computed detection efficiency which arises from the poorly known shape factors for the  $\beta$  spectrum and the incertitude associated with the ionization quenching function used in the CN2003 tracing code. Next, is the propagated standard uncertainty (0.39%) resulting from the 0.03 uncertainty interval in the decay probability for both  $^{210}\text{Pb}$   $\beta$  transitions. The third (0.35%) is the standard uncertainty for uncorrected, potential cocktail instability and mismatch effects (Collé, 1997b). All remaining components have standard uncertainties of less than 0.07% and in combination make only a 0.14% contribution to the 1.2% combined standard uncertainty.

## 2.5. Confirmatory measurements

The intent of any confirmatory measurement as performed by our laboratory is to ensure that the standardization result is confirmed by supplementary measurements that are completely independent of the primary method. Employment of such an independent confirmatory measurement, even if it is substantially less accurate, is a vital aspect of our SRM standardization work. Three confirmatory approaches were used here; viz., (i) HPGe  $\gamma$ -ray spectrometry, (ii)  $2\pi\alpha$  spectrometry of  $^{210}\text{Po}$  and (iii)  $4\pi\beta(\text{LS})-\gamma(\text{NaI})$  anticoincidence counting.

### 2.5.1. HPGe $\gamma$ -ray spectrometry

For confirmatory purposes, attempts were made to assay the  $^{210}\text{Pb}$  activity content of the SRM ampoules by HPGe

$\gamma$ -ray spectrometry. The two detectors employed for these measurements were noted in Section 2.3. To maintain independence, even though no previous primary standardization by NIST for  $^{210}\text{Pb}$  exists, none of the efficiency curves used for these measurements incorporated a value for the  $^{210}\text{Pb}$  46.54 keV  $\gamma$ -ray.

Five 24-hour-long measurements with the X detector (three at a “side mount” geometry and two at 25 cm) resulted in an average massic activity of  $(9.22 \pm 0.46) \text{ kBq g}^{-1}$  (at the 15 June 2006 reference time); whereas five measurements with the B detector (three at 35 cm and two at 25 cm) had an average of  $(9.72 \pm 0.63) \text{ kBq g}^{-1}$ . The cited uncertainties correspond to  $k = 2$  intervals for the expanded combined standard uncertainty. The internal relative standard deviations on the two sets of five measurements were 0.42% and 2.4%, respectively. Combination of both sets of measurements resulted in a massic activity value of  $9.466 \text{ kBq g}^{-1}$ , with a relative  $k = 2$  standard uncertainty of 5.8%. This laboratory’s methodology for uncertainty assessments for these  $\gamma$ -ray measurements has been treated by Pibida et al. (2006). The somewhat low decay probability (4.25%) and low energy of the sole  $^{210}\text{Pb}$  46.54 keV  $\gamma$ -ray (located on the steep upward side of an efficiency curve) largely precluded a more accurate determination. This  $\gamma$ -ray spectrometry result is biased from the primary LS-based result by +4.7%. Hence, although the two results differ substantially, they can be considered to be in agreement within the large uncertainty on the  $\gamma$ -ray spectrometry value.

### 2.5.2. $2\pi\alpha$ spectrometry of $^{210}\text{Po}$

The second confirmatory measurement approach employed alpha spectrometry of  $^{210}\text{Po}$ , the  $^{210}\text{Pb}$  granddaughter, after separation from the  $^{210}\text{Pb}$  SRM solution. The separation procedure, based on the spontaneous



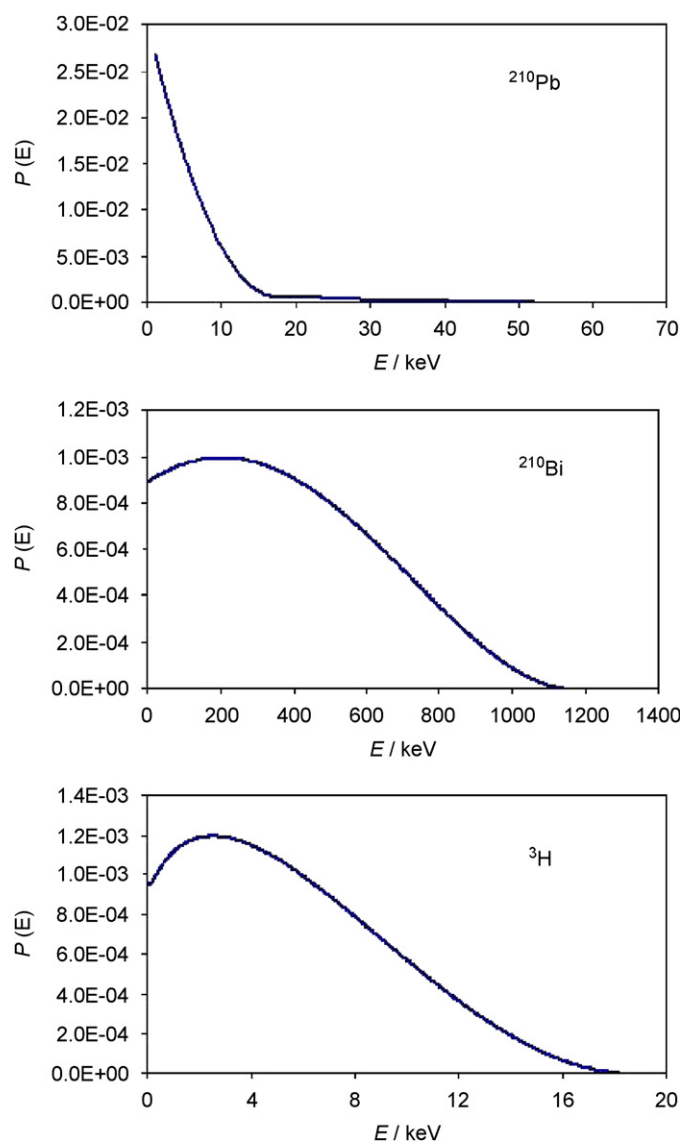


Fig. 6. Theoretical beta spectra for  $^{210}\text{Pb}$ ,  $^{210}\text{Bi}$ , and  $^3\text{H}$ , given by the probability  $P(E)$  of a  $\beta^-$  particle of energy  $E$  as a function of  $E$  (in units of keV). The spectra are normalized such that the integral of  $P(E)$  over all  $E$  is unity.

deposition of polonium on silver, consisted of the following sequence. (1) The  $^{210}\text{Pb}$  solution was diluted by a factor of about 60 with a  $1\text{ mol L}^{-1}\text{ HNO}_3$  solution. (2) An aliquant of a  $^{209}\text{Po}$  solution, SRM 4326 (NIST, 1995), was gravimetrically added as the polonium tracer. (3) A few milliliters of concentrated  $\text{HNO}_3$  acid were added to the sample and it was evaporated to dryness. (4) The sample was then re-dissolved in  $0.5\text{ M HCl}$  acid. (5) About  $1\text{ mL}$  of saturated hydrazine hydrochloride was added, and the sample was transferred to a  $30\text{ mL}$  polyethylene bottle. (6) Silver discs,  $18\text{ mm}$  diameter, were placed in the caps of each bottle. (7) The bottles were inverted so that the silver discs were covered by the sample solution. (8) The bottles were heated, while upside down, in a water bath at  $60^\circ\text{C}$  for  $4\text{ h}$  to allow polonium to be spontaneously deposited on the silver. (9) After  $4\text{ h}$ , the silver discs were removed, and

rinsed with water and alcohol. (10) The deposited sources were then covered with thin films ( $10\text{--}30\text{ }\mu\text{g cm}^{-2}$ , prepared from a 1:1 by volume mixture of isoamyl acetate and flexible colloidion) to prevent contamination of the detectors.

Two  $^{210}\text{Pb}$  samples and two blanks were measured overnight by alpha spectrometry with Si surface barrier detectors. The reagent blanks were obtained using the lead carrier solution and diluted similarly (by a factor of about 60) to that for the  $^{210}\text{Pb}$  samples.

The resultant alpha spectra were analyzed and the activity of  $^{210}\text{Po}$  was determined and corrected for decay from the time when polonium was separated from lead by its spontaneous deposition onto the silver sources. The  $^{210}\text{Po}$  yield and detection efficiency was determined from the spectral yield of the  $^{209}\text{Po}$  tracer. The  $^{210}\text{Pb}$  activity, in turn, was calculated by assuming that  $^{210}\text{Pb}$  and  $^{210}\text{Po}$  were in radioactive equilibrium in the original SRM solution. No polonium was detected in the blanks. The  $^{210}\text{Pb}$  massic activity (on application of the aliquant masses) from two replicate samples was determined to be  $8.77\text{ kBq g}^{-1}$  (as of 1200 EST 15 June 2006). The two determinations agreed to within  $0.2\%$ . A canonical standard uncertainty for this measurement process is approximately  $2\%$  at  $k = 2$ . This massic activity value differs from the LS-based result by  $-3.0\%$ , but is very dependent on the 10-year decay correction for the  $^{209}\text{Po}$  used as a tracer. The widely adopted value of  $(102 \pm 5)\text{ a}$  for the  $^{209}\text{Po}$  half-life (Martin, 1991; Kondev, 2004; ENSDF, 2006) is suspected to be in error by a large factor (Collé et al., 2007a). Based on decay data from two separate primary standardizations of a  $^{209}\text{Po}$  solution standard conducted 12 years apart, an estimated half-life of about  $128\text{ a}$  was observed. Re-analysis of the present spectrometry data, assuming the longer half-life of  $128\text{ a}$ , results in a  $^{210}\text{Pb}$  massic activity of  $8.92\text{ kBq g}^{-1}$ , which differs from the LS-based activity by only  $-1.3\%$ . This agreement in fact served as part of the evidence that justifies the need for a longer  $^{209}\text{Po}$  half-life (Collé et al., 2007a).

#### 2.5.3. $4\pi\beta(\text{LS})\text{--}\gamma(\text{NaI})$ anticoincidence counting

A confirmatory determination of the  $^{210}\text{Pb}$  SRM solution was also performed by live-timed  $4\pi\beta(\text{LS})\text{--}\gamma(\text{NaI})$  anti-coincidence counting with efficiency extrapolation. The method has been described by Baerg et al., (1976). Lucas (1998) described the counting system used at NIST, as well as its application. The counting system uses LS sources in glass pseudo-hemispherical vials, having a radius of approximately  $1.5\text{ cm}$  and an internal volume of about  $8\text{ mL}$ . The  $4\pi\beta$  counting channel consists of this source coupled onto a suitable photomultiplier tube. A “4 in-5 in” ( $10\text{ cm} \times 13\text{ cm}$ )  $\text{NaI(Tl)}$  well counter with a “2.5 in” ( $6.4\text{ cm}$ ) well that surrounds the vial serves as the  $\gamma$  channel. The characteristics of the hemispherical sources used for the present measurements are described in Table 1.

The nuclide  $^{210}\text{Pb}$  is a good case for this anticoincidence counting method because the LS efficiency is already over

Table 3

Uncertainty analysis for the  $^{210}\text{Pb}$  massic activity of SRM 4337, standardized by  $4\pi\alpha\beta$  LS counting with  $^3\text{H}$ -standard efficiency tracing

Uncertainty component		Assessment type <sup>a</sup>	Relative uncertainty (%)
1	LS within-measurement-occasion precision; typical standard deviation of the mean for 7–11 sources measured 3–5 times on one occasion; values ranged from 0.007 to 0.056%	A	0.03
2	LS-between-measurement-occasion precision; reproducibility in massic activity for 3–5 replicate measurements of 7–11 sources in three measurement series with three counters on two to three measurement occasions; standard deviation of the mean for $\nu = 443$ degrees freedom	A	0.067
3	Background LS measurement variability; wholly embodied in components 1 and 2	A	—
4	Scintillator dependences; wholly embodied in components 1 and 2	A	—
5	LS cocktail stability and composition mismatch effect	B	0.35
6	Gravimetric (mass) measurements for LS sources and for $^3\text{H}$ standard dilution	B	0.07
7	Live time determinations for LS counting time intervals, includes uncorrected dead time effects	B	0.06
8	Decay corrections for $^{210}\text{Pb}$	B	0.002
9	Decay corrections for $^3\text{H}$	B	0.0005
10	Limit for photon-emitting impurities	B	0.02
11	Beta endpoint energy, $E_{\beta(\text{max})}$ , for $^{210}\text{Pb}$ for an uncertainty of 0.5 keV	B	0.033
12	Beta decay branching ratios for $^{210}\text{Pb}$ for an uncertainty of 0.03	B	0.39
13	$E_{\beta(\text{max})}$ for $^{210}\text{Bi}$ for an uncertainty of 1.5 keV	B	0.001
14	Computed LS detection efficiency for $^{210}\text{Pb}$	B	1.1
15	Computed LS detection efficiency for $^{210}\text{Bi}$	B	0.04
16	Assumed $\alpha$ detection efficiency for $^{210}\text{Po}$ , including extrapolation to zero energy	B	0.05
Relative combined standard uncertainty			1.2
Relative expanded uncertainty ( $k = 2$ )			2.4

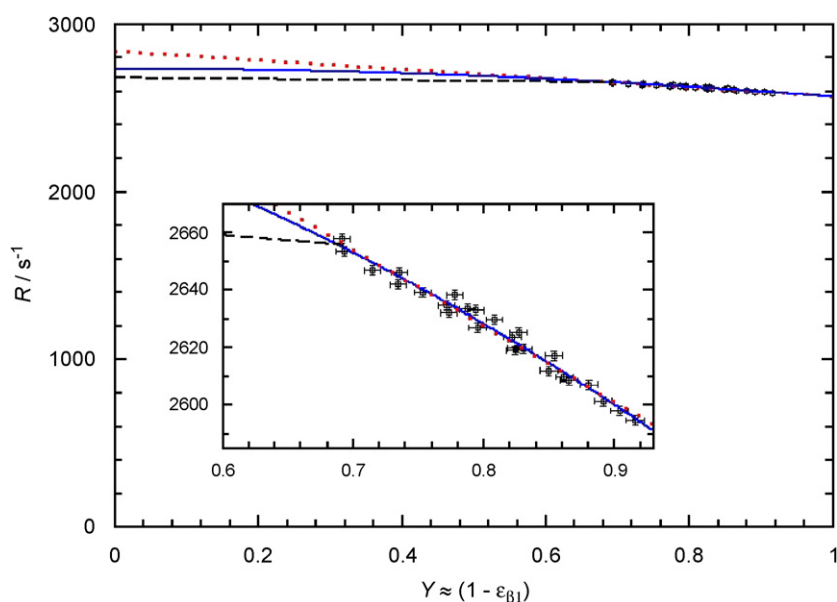
<sup>a</sup>A, denotes evaluation by statistical methods; B, denotes evaluation by other methods.

Fig. 7. Typical  $4\alpha\beta\text{--}\gamma$  anticoincidence data extrapolation, given by the LS counting rate  $R$  of a source (in units of  $\text{s}^{-1}$ ) as a function of the anticoincidence to singles- $\gamma$  ratio  $Y$ . The zero intercept corresponds to the total particle emission rate of the solution. Each point corresponds to that obtained for 1000 s livetime. The solid (blue) line is a quadratic fit. The dotted (red) line is a linear fit, which is expected to be an upper limit. The dashed (black) line is an extrapolation of only the measured efficiency for  $\beta_1$  and provides a lower limit on the intercept (see the text). The inset shows the data region, whose uncertainty intervals correspond to statistical standard deviations.

95% before the extrapolation begins (see Fig. 7). In the case of the present  $^{210}\text{Pb}$  measurements, the LS detection efficiency,  $\varepsilon$ , for the lowest-energy  $\beta$  branch ( $\beta_1$ ; 17.0 keV endpoint energy) was traced using the 46.539-keV unconverted  $\gamma$ -ray whose emission probability is 4.25%. Refer to the decay scheme in Fig. 1. The anticoincidence to

singles- $\gamma$  ratio,  $Y$ , is then a measure of  $(1 - \varepsilon_{\beta_1})$ . The LS efficiency was varied by adjusting the low-energy detection threshold and the LS rate was extrapolated to  $Y = 0$  (i.e.,  $\varepsilon_{\beta_1} = 1$ ). Since the  $\beta_1$  endpoint energy is much lower than that of the other  $\alpha$  and  $\beta$  particles emitted by the solution, it was assumed that at  $\varepsilon_{\beta_1} = 1$ , the LS efficiency for the other

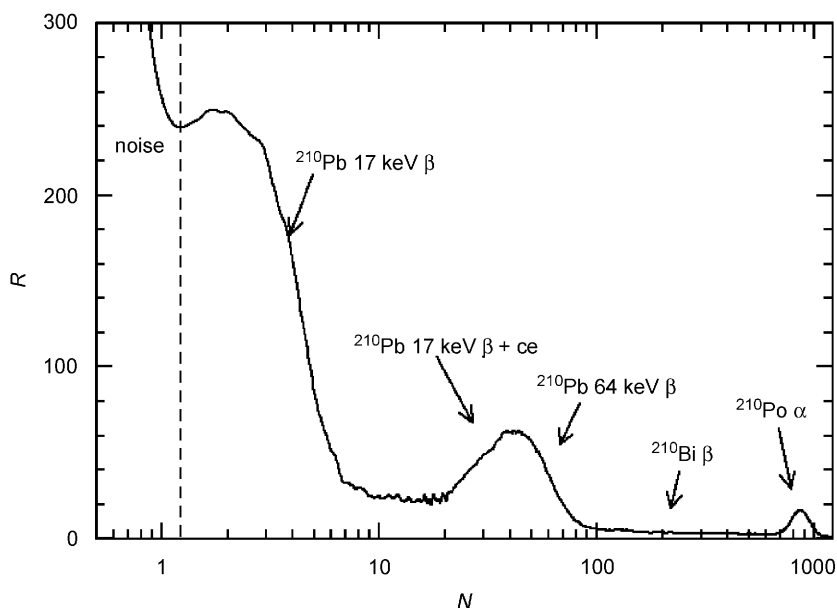


Fig. 8. Typical LS spectrum of a  $^{210}\text{Pb}$  source as obtained with the  $4\alpha\beta\text{-}\gamma$  anticoincidence counting system, in terms of the counting rate  $R$  (without background subtraction and arbitrarily normalized) versus spectral channel number  $N$ . The spectrum was made by overlaying data taken at three different amplifier gains, to cover a large energy range in detail. Note the logarithmic horizontal axis, which distorts the apparent spectrum because the energy width ( $E_i - E_{i+1}$ ) of each channel  $\Delta N$  is increasingly larger, given by the logarithmic energy difference  $\Delta N = \log(E_i/E_{i+1})$ . The lowest energy component of the spectrum is the  $^{210}\text{Pb}$  17-keV  $\beta_1$  branch from  $^{210}\text{Pb}$ , which sits on the tails of the other components and extends down into single-photon and noise peaks.

decays will also be unity (see Fig. 8). If  $\beta_1$  were the only component of the LS spectrum, then a linear extrapolation to  $Y = 0$  would be expected (Baerg et al., 1976). However, the presence of the other components in the LS spectrum, particularly the strong peak corresponding to  $\beta_1$  and the conversion electron in coincidence at about 45 keV (most likely  $^{210}\text{Pb}$  decay mode), are expected to lead to a quadratic extrapolation. This effect is predicted by various models of the LS spectrum, and is well known from studies of other  $\beta$  emitters with converted  $\gamma$ -rays and/or multiple  $\beta$  transitions (Baerg, 1981).

The challenge in applying this method to the present  $^{210}\text{Pb}$  measurements was that the lower-level discriminator window on the LS spectrum was limited by detector noise to roughly 8 keV  $\beta$  energy, which encompassed about 32% of the  $\beta_1$  spectrum. Thus, the extrapolation to  $\varepsilon_{\beta_1} = 1$  covers a range twice as long as the data set. This adds considerable uncertainty to the functional form of the extrapolation. The only constraint that was placed on the quadratic fit in Fig. 7, was that the curve not turn over before reaching  $Y = 0$ , which would be physically impossible since the total LS rate cannot decrease as  $\varepsilon_{\beta_1}$  increases. A linear extrapolation, also shown in Fig. 7, can be considered an upper limit of the particle emission rate, and leads to an intercept close to the upper 95.4% confidence limit of the quadratic fit. A model-independent, lower limit is determined by using the highest LS efficiency data point measured, and scaling it slightly for the measured  $\varepsilon_{\beta}$ . (The adjustment is small because only 4% of  $\beta_1$  events occur without a chance to sum with a conversion electron and only 33% of the total LS rate is

from  $^{210}\text{Pb}$ .) The resulting linear intercept does not account for the subunity efficiencies for the other  $\beta$  transitions and possibly even the detected  $\alpha$  decay events, so it is certainly an underestimate of the particle-emission rate.

The  $^{210}\text{Pb}$  activity was calculated from the massic particle-emission rate under the assumption of secular equilibrium for the  $^{210}\text{Pb}$  decay series. In this way, the upper limit from the linear fit and the lower limit from the scaling of the data for only the 17 keV  $\beta_1$  gave a range of massic activities of  $8.882\text{--}9.407\text{ kBq g}^{-1}$ . Taking this range to be a 100% uncertainty interval for a rectangular distribution and combining the resultant standard uncertainty with the other ( $<0.6\%$ ) sources of uncertainty, leads to a massic activity value with expanded uncertainty ( $k = 2$ ) of  $(9.10 \pm 0.30)\text{ kBq g}^{-1}$ .

This massic activity value agrees with that of the LS-based primary standardization to about 0.7%. Nevertheless, it was not deemed suitable for contributing directly to the certified value of SRM 4337, due to the unacceptably large range of extrapolation and the significant (2%) disagreement between the linear and quadratic fits. Moreover, there is not strong enough justification for using a quadratic fit over such a large range. Future improvements in the low energy  $\beta$  efficiency and signal-to-noise ratio should lead to better estimates for the massic activity.

### 3. Summary

The  $^{210}\text{Pb}$  radioactivity solution standards were certified and will be disseminated as NIST SRM 4337 with the following specifications:

Table 4

Comparison of the confirmatory measurement results with the certified value for the  $^{210}\text{Pb}$  massic activity  $A$  of SRM 4337 as obtained from the  $4\pi\alpha\beta$  LS-based standardization

Method	$A/\text{kBq g}^{-1}$	$U (k = 2)/(\%)$	Difference/(%)
$4\pi\alpha\beta$ LS meas. (CNET)—certified value	9.037	2.4	—
HPGe $\gamma$ -ray spectrometry	9.47	5.8	+4.7
$2\pi\alpha$ spectrometry of $^{210}\text{Po}$ (102 a $^{209}\text{Po}$ )	8.77	$\approx 2$	−3.0
$2\pi\alpha$ spectrometry of $^{210}\text{Po}$ (128 a $^{209}\text{Po}$ )	8.92	$\approx 2$	−1.3
$4\pi\beta$ - $\gamma$ anticoincidence counting	9.10	3.3	+0.7

All massic activity values are for a reference time of 1200 EST, 15 June 2006.

*Form:* Solution of nominal  $1 \text{ mol L}^{-1} \text{ HNO}_3$  with  $11 \mu\text{g Pb}^{2+}$  and  $21 \mu\text{g Bi}^{3+}$  per gram of solution in a flame-sealed NIST 5 mL borosilicate glass ampoule.

*Solution mass:*  $(5.133 \pm 0.002) \text{ g}$ .

*Solution density:*  $(1.028 \pm 0.002) \text{ g mL}^{-1}$  at  $20^\circ \text{C}$ .

*Reference time:* 1200 EST, 15 June 2006.

*Massic activity:*  $9.037 \text{ kBq g}^{-1}$ .

*Relative expanded ( $k = 2$ ) uncertainty:* 2.4%.

The standardization was based on  $4\pi\alpha\beta$  liquid scintillation (LS) measurements with  $^3\text{H}$ -standard efficiency tracing using the CIEMAT/NIST method with the CN2003 code of Gunther (2003). The mean massic activity was obtained from 444 determinations, as derived from measurements using three different LS counters with a total of 25 differently quenched LS cocktails. The cocktails were made with two different scintillators in three different cocktail composition series and were measured on multiple occasions over periods of up to 30 days. The large 2.4% uncertainty on the certified  $^{210}\text{Pb}$  massic activity, somewhat abnormal for radioactivity standardizations by this laboratory, devolves from the uncertainty associated with the appropriateness of the ionization quenching function used in the tracing codes to compute the LS detection efficiencies.

Confirmatory measurements for the  $^{210}\text{Pb}$  massic activity of SRM 4337 were performed by three alternative methods. A comparison of their results with the  $4\pi\alpha\beta$  LS-based standardization result is summarized in Table 4. As indicated all of these confirmations are in agreement with the certified massic activity value within the respective methods' rather large estimated uncertainties. It may be of interest to note that the unweighted mean and propagated ( $k = 2$ ) uncertainty of the two "best" determinations (viz., the  $2\pi\alpha$  spectrometry of  $^{210}\text{Po}$  with 128 a  $^{209}\text{Po}$  and the  $4\pi\beta$ - $\gamma$  anticoincidence counting) is  $(9.01 \pm 0.024) \text{ kBq g}^{-1}$ , which agrees with the certified LS-based value to within 0.3%.

This work constitutes the first primary standardization of  $^{210}\text{Pb}$  by NIST, the national metrology laboratory of the USA. The availability of the resultant  $^{210}\text{Pb}$  solution standard, SRM 4337, will be welcomed by the worldwide environmental radioactivity measurement community.

## Acknowledgment

Dr. Brian E. Zimmerman of the NIST Radioactivity Group is thanked for his ever-helpful assistance in getting computer codes to work and for his commentaries and occasional insights on LS counting.

## References

- American National Standards Institute (ANSI), 1999. American National Standard for Calibration and Use of Germanium Spectrometers for the Measurement of Gamma-Ray Emission Rates of Radionuclides, ANSI N42.14-1999, Washington, DC.
- Bateman, H., 1910. The solution of a system of differential equations occurring in the theory of radioactive transformations, Proc. Cambridge Phil. Soc. 15, 423–427.
- Baerg, A.P., 1981. Multiple channel  $4\pi\beta$ - $\gamma$  anticoincidence counting. Nucl. Instr. Meth. 190, 345–349.
- Baerg, A.P., Munzenmayer, K., Bowes, G.C., 1976. Live-timed anticoincidence counting with extending dead-time circuitry. Metrologia 12, 77–80.
- Behrens, H., Szybisz, L., 1976. Shapes of Beta Spectra, Physik Daten Rpt No. ZAED-6-1, Zentralstelle für Atomkernenergie-Dokumentation, Kernforschungszentrum Karlsruhe, FRG (unpublished).
- Cassette, P., 2002. Evaluation of the influence of wall effects on the liquid scintillation counting detection efficiency for the standardization of high energy beta and alpha radionuclides. In: Mobius, S., Noakes, J.E., Schonhofer, F. (Eds.), LSC 2001. Advances in Liquid Scintillation Spectrometry. Radiocarbon, University of Arizona, Tucson, AZ, USA, pp. 45–55.
- Cassette, P., 2006. Laboratoire National Henri Becquerel (CEA, Gif sur Yvette, France), private communications on BETAENG6 code. (see also Cassette, P., SPECBETA programme de calcul du spectre en énergie des électrons émis par des radionucléides émetteurs beta, CEA Rpt, 1992.)
- Chechev, V.P., 2006.  $^3\text{H}$  data, online update by Laboratoire National Henri Becquerel of Table of Radionuclides. In: Bé, M.M., et al. (Eds.), Bureau International des Poids et Mesures (Sèvres, France). Refer to [http://www.nucleide.org/DDEP\\_WG/DDEPdata.htm](http://www.nucleide.org/DDEP_WG/DDEPdata.htm)
- Collé, R., 1997a. A simple transform to linearize and resolve two-component decay data: illustration of its use and efficacy in assaying  $^{32}\text{P}/^{33}\text{P}$  mixtures by liquid scintillation counting. Radioact. Radiochem. 8 (2), 5–18.
- Collé, R., 1997b. Cocktail mismatch effects in  $4\pi\beta$  liquid scintillation spectrometry: implications based on the systematics of  $^3\text{H}$  detection efficiency and quench indicating parameter variations with total cocktail mass (volume) and  $\text{H}_2\text{O}$  fraction. Appl. Radiat. Isot. 48, 833–842.
- Collé, R., 1997c. Systematic effects of total cocktail mass (volume) and  $\text{H}_2\text{O}$  fraction on  $4\pi\beta$  liquid scintillation spectrometry of  $^3\text{H}$ . Appl. Radiat. Isot. 48, 815–883.



- Collé, R., 1999. Chemical digestion and radionuclidic assay of TiNi-encapsulated  $^{32}\text{P}$  intravascular brachytherapy sources. *Appl. Radiat. Isot.* 50, 811–833.
- Collé, R., 2000. On the radioanalytical methods used to assay stainless-steel-encapsulated, ceramic-based  $^{90}\text{Sr}$ – $^{90}\text{Y}$  intravascular brachytherapy sources. *Appl. Radiat. Isot.* 52, 1–18.
- Collé, R., 2001. Calibration of  $^{32}\text{P}$  “hot-wall” angioplasty-balloon-catheter sources by liquid-scintillation-spectrometry-based destructive radionuclidic assays. *Appl. Radiat. Isot.* 54, 611–622.
- Collé, R., Zimmerman, B.E., 1996a. Nickel-63 standardization: 1968–1995. *Radioact. Radiochem.* 7 (2), 12–27.
- Collé, R., Zimmerman, B.E., 1996b.  $^{63}\text{Ni}$  Half-Life: a new experimental determination and critical review. *Appl. Radiat. Isot.* 47, 677–691.
- Collé, R., Zimmerman, B.E., 1997. A Compendium on the NIST radionuclidic assays of the massic activity of  $^{63}\text{Ni}$  and  $^{55}\text{Fe}$  solutions used for an international intercomparison of liquid scintillation spectrometry techniques. *J. Res. Natl. Inst. Stds. Tech.* 102, 523–549.
- Collé, R., Laureano-Pérez, L., Outola, I., 2007a. A note on the half-life of  $^{209}\text{Po}$ . *Appl. Radiat. Isot.* 65, 728–730.
- Collé, R., Zimmerman, B.E., Cassette, P., Laureano-Pérez, L., 2007b.  $^{63}\text{Ni}$ , its half-life and standardization: revisited. *Appl. Radiat. Isot.*, in press, doi:10.1016/j.apradiso.2007.07.017.
- Coursey, B.M., Grau Malonda, A., Garcia-Torano, E., Los Arcos, J.M., 1985. Standardization of pure-beta-particle-emitting radionuclides. *Trans. Am. Nucl. Soc.* 50, 13–15.
- Coursey, B.M., Mann, W.B., Grau Malonda, A., Garcia-Torano, E., Los Arcos, J.M., Gibson, J.A.B., Reher, E., 1986. Standardization of C-14 by  $4\pi\beta$  liquid scintillation efficiency tracing with hydrogen-3. *Appl. Radiat. Isot.* 37, 403.
- Dataplot, 2007. Dataplot is a free, public-domain, multi-platform software system for scientific visualization, statistical analysis, and non-linear modeling. It was developed at the National Institute of Standards and Technology (Gaithersburg, MD, USA) and is available on-line at <<http://www.itl.nist.gov/div898/software/dataplot/>>.
- Evaluated Nuclear Structure Data File (ENSDF), 2006. Online database, National Nuclear Data Center, Brookhaven Laboratory (Upton, NY), October 2006. Refer to <<http://www.nndc.bnl.gov/ensdf/>>.
- Garcia-Torano, E., 1993. Centro de Investigaciones Energéticas, Medioambientales y Tecnológicas (CIEMAT), private communication on EFFY4.
- Garcia-Torano, E., Grau Malonda, A., 1985. Effy, a new program to compute the counting efficiency of beta particles in liquid scintillators. *Comput. Phys. Commun.* 36, 307–312.
- Grau Malonda, A., 1999. Free Parameter Models in Liquid Scintillation Counting, Centro de Investigaciones Energéticas, Medioambientales y Tecnológicas (CIEMAT), Madrid, Spain, p.23.
- Grau Malonda, A., Garcia-Torano, E., 1982. Evaluation of counting efficiency in liquid scintillation counting of pure  $\beta$ -ray emitters. *Int. J. Appl. Radiat. Isot.* 33, 249–253.
- Grau Malonda, A., Garcia-Torano, E., Los Arcos, J.M., 1985. Liquid scintillation counting efficiency as a function of figure of merit for pure beta-particle emitters. *Int. J. Appl. Radiat. Isot.* 2, 157–158.
- Gunther, E., 2002. Determination of the activity of radionuclidic sources emitting beta and gamma radiation using the CIEMAT/NIST method. In: Mobius, S., Noakes, J.E., Schonhofer, F. (Eds.), *LSC 2001, Advances in Liquid Scintillation Spectrometry*. Radiocarbon, University of Arizona, Tucson, AZ, USA, pp. 57–63.
- Gunther, E., 2003. Physikalisch-Technische Bundesanstalt (Braunschweig, Germany), private communication.
- International Organization for Standardization (ISO), 1993. Guide to the Expression of Uncertainty in Measurement (corrected and reprinted, 1995). ISO, Geneva.
- Kondev, F.G., 2004. Nuclear data sheets for  $A = 205$ . *Nucl. Data Sheets* 101, 586.
- Los Arcos, J.M., Ortiz, F., 1997. kB: a code to determine the ionization quenching function  $Q(E)$  as a function of the kB parameter. *Comput. Phys. Commun.* 103, 83–94.
- Los Arcos, J.M., Grau Malonda, A., Fernandez, A., 1987. Viaskl: a computer program to evaluate the liquid scintillation counting efficiency and its associated uncertainty for K-L-atomic-shell electron-capture nuclides. *Comput. Phys. Commun.* 44, 209–220.
- Lucas, L.L., 1998. Calibration of the massic activity of a solution of  $^{99}\text{Tc}$ . *Appl. Radiat. Isot.* 49, 1061–1064.
- Lucas, L.L., 2005. National Institute of Standards and Technology, Gaithersburg, MD, USA, private communications and internal NIST records.
- Martin, M., 1991. Nuclear data sheets for  $A = 205$ . *Nucl. Data Sheets* 63, 723.
- Michotte, C., 2006. Bureau International des Poids et Mesures (Sèvres, France), Private communications on SIMPBETA code. (see also Michotte, C., Beta spectrum shape calculation based on Behrens and Janeke Tables, BIPM Rpt., unpublished, 2006).
- National Institute of Standards and Technology (NIST), 1995. Certificate for Standard Reference Material 4326, Polonium-209 Radioactivity Standard. NIST, Gaithersburg, MD, USA issued January 1995; revised December 2005.
- National Institute of Standards and Technology (NIST), 2000. Certificate for Standard Reference Material 4927F, Hydrogen-3 Radioactivity Standard. NIST, Gaithersburg, MD, USA issued June 1999; revised October 2000.
- National Institute of Standards and Technology (NIST), 2006. Certificate for Standard Reference Material 4337, Lead-210 Radioactivity Standard. NIST, Gaithersburg, MD, USA issued November, 2006.
- National Institute of Standards and Technology (NIST), 2007. Refer to <<http://physics.nist.gov/Divisions/Div846/srm.html>> for the standardized SRM ampoule dimensions, Gaithersburg, MD, USA.
- Pibida, L., Hsieh, E., Fuentes-Figueroa, A., Hammond, M.M., Karma, L., 2006. Software studies for germanium detector data analysis. *Appl. Radiat. Isot.* 64, 1313–1318.
- Pibida, L., Nafee, S.S., Unterweger, M., Hammond, M.M., Karma, L., Abbas, M.I., 2007. Calibration of HPGe gamma-ray detectors for measurement of radioactive noble gas sources. *Appl. Radiat. Isot.* 65, 225–233.
- Snedecor, G.W., Cochran, W.G., 1967. *Statistical Methods*, sixth ed. Iowa State University Press, Ames, IA, USA, p.299ff.
- Taylor, B.N., Kuyatt, C.E., 1994. Guidelines for Evaluating and Expressing the Uncertainty of NIST Measurement Results, NIST Technical Note 1297, National Institute of Standards and Technology, Gaithersburg, MD, USA. Available from the Superintendent of Documents, US Government Printing Office, Washington, DC, USA.
- Zimmerman, B.E., Collé, R., 1997a. Cocktail volume effects in  $4\pi\beta$  liquid scintillation spectrometry with  $^3\text{H}$ -standard efficiency tracing for low-energy  $\beta$ -emitting radionuclides. *Appl. Radiat. Isot.* 48, 365–378.
- Zimmerman, B.E., Collé, R., 1997b. Standardization of  $^{63}\text{Ni}$  by  $4\pi\beta$  liquid scintillation spectrometry with  $^3\text{H}$ -standard efficiency tracing. *J. Res. Natl. Inst. Stds. Tech.* 102, 455–477.